ANIMAL CELLS AND SYSTEMS
2025, VOL. 29, NO. 1, 251–263
https://doi.org/10.1080/19768354.2025.2492148

Taylor & Francis
Taylor & Francis Group

Establishment of an *in vitro* erythroid differentiation system from canine peripheral blood mononuclear cells

Sung Ah Park[a], Arim Shin[a], Eunji Im[b], Do Hyeon Yu[c], Minji Kim[c], Chul Geun Kim[d] and Eun Jung Baek[a,b,e]

[a]Department of Translational Medicine, Graduate School of Biomedical Science & Engineering, Hanyang University, Seoul, Korea; [b]Department of Research and Development, ArtBlood Inc., Seoul, Korea; [c]College of Veterinary Medicine, Gyeongsang National University, Jinju, Korea; [d]Department of Life Science, Hanyang University, Seoul, Korea; [e]Department of Laboratory Medicine, College of Medicine, Hanyang University, Seoul, Korea

ABSTRACT

Blood transfusion is a critical, lifesaving medical procedure for dogs. However, the limited availability of blood donors and ethical concerns highlight the need for alternative solutions, such as *in vitro*-produced red blood cells (RBCs), which remain unexplored in canines. This study aimed to produce canine erythrocytes *in vitro* from peripheral blood (PB) mononuclear cells (MNCs), optimize culture conditions using either human or canine reagents, and identify relevant cell markers. Results indicated that canine erythropoiesis can be induced by human or canine cytokines, producing RBCs within approximately 20 days. Although cell numbers decreased during the first seven days, immature erythroid cells proliferated, reaching peak expansion and RBC production by day 17. Despite the smaller cell size of the cultured RBCs than that of humans, the morphology at each stage of erythroid maturation was analogous to that of human erythropoiesis. Furthermore, the expression patterns of canine alpha hemoglobin stabilizing protein and erythropoietin receptor mirrored those observed in human erythropoiesis. Oxygen-hemoglobin (oxygen-Hb) association and dissociation curves of cultured RBCs closely resembled those of native canine RBCs, indicating an appropriate oxygen-carrying capacity. This study presents the first evidence of successful *in vitro* production of canine RBCs, offering a promising tool for research and potential therapeutic applications.

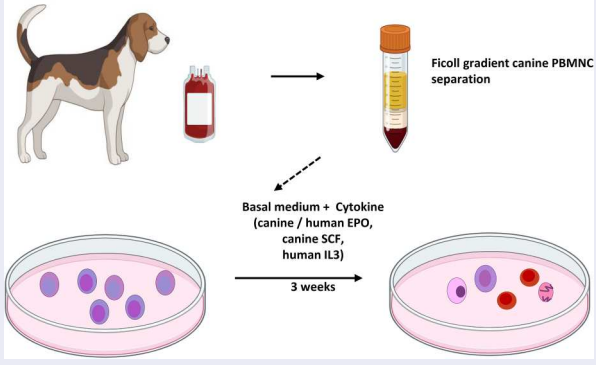

ARTICLE HISTORY
Received 13 February 2025
Accepted 11 March 2025

KEYWORDS
Canine blood; erythrocyte; *in vitro* culture; erythropoietin

Introduction

Red blood cells (RBCs) are the most abundant cells in the body and play a critical role in delivering oxygen to tissues. In veterinary medicine, blood transfusions in dogs is essential for managing anemia and acute blood loss caused by trauma or surgical procedures. Currently, blood transfusions rely exclusively on donor animals. However, as advanced veterinary critical care has become more common, the demand for blood products has risen substantially. The limited availability of donor animals and ethical concerns surrounding their use underscore the need for alternative solutions such as *in vitro*-produced RBCs.

Despite the increased demand for canine RBCs, basic research on their production has not been fully explored. The main challenges faced during their development

CONTACT Eun Jung Baek doceunjung@hanyang.ac.kr Department of Laboratory Medicine, College of Medicine, Hanyang University, 153, Gyeongchun-ro, Guri-si, Gyeonggi-do 11923, Korea

include the scarcity of reagents and a lack of information regarding the suitability of the culture media. Most studies on canine mononuclear cells (MNCs) have primarily focused on immune cells, aiming to understand immune responses and cellular functions in various contexts (Neuner et al. 1997; Niemeyer et al. 2001; Suter et al. 2004; Lee et al. 2018). Conversely, the *in vitro* production of human RBCs has been extensively studied for years due to a shortage of blood donations, and clinical trials are currently underway. Neildez-Nquyen et al. first demonstrated that cord blood (CB)-derived hematopoietic stem/progenitor cells (HSPCs) could expand nearly a million-fold, though with a low enucleation rate (Neildez-Nguyen et al. 2002).

Subsequent studies have introduced combinations of specific erythropoietic cytokines and culture methods to better replicate the bone marrow microenvironment, thereby enhancing HSPC expansion, differentiation, and enucleation *in vitro*. For instance, Lee et al. achieved an 80% enucleation rate by culturing erythroid cells in 400 μm diameter microporous microcarriers, which allowed for high cell densities (Lee et al. 2015). Similarly, Han et al. produced mature biconcave erythrocytes by culturing cells in a bioreactor, identifying optimal culture parameters for cell differentiation using a design of experiments (DOE) approach (Han et al. 2021). In 2011, Giarratana et al. reported a breakthrough by successfully transfusing 2 mL of cultured blood into a human recipient using autologous CD34+ cells (Giarratana et al. 2011). More recently, the Recovery and Survival of Stem Cell-Originated Red Cells (RESTORE) clinical trial in the UK attempted blood transfusion using laboratory-grown RBCs (Kutikuppala et al. 2023).

Research on *in vitro* erythropoiesis using canine models emerged in the 1970s, initially focusing on cell cultures in enriched methylcellulose media. This method was first developed to produce erythroid colonies from mouse fetal liver hematopoietic cells in an erythropoietin (EPO)-dependent manner (Stephenson et al. 1971), and was later adapted for canine models. Colonies of Hb-synthesizing cells were successfully generated from canine bone marrow (BM) cells cultured in the presence of EPO partially purified from anemic sheep plasma (Popovic et al. 1977). In this system, colony formation was directly proportional to the logarithm of EPO concentration. Subsequent studies aimed to improve erythroid colony production by supplementing cultures with β-adrenergic agonists (Brown and Adamson 1977a), cyclic nucleotides (Brown and Adamson 1977b), and thyroid hormones (Popovic et al. 1977).

In addition to its enhancing effects on mesenchymal stem cell proliferation and homing ability (Zhou et al. 2018; Lykov et al. 2020; El Mahdy et al. 2023), EPO is critical for maintaining optimal RBC mass and ensuring sufficient oxygen delivery to tissues (Haase 2010). Research has shown that canine serum EPO is more effective than human urinary EPO, when used in comparable concentrations, at stimulating the colony-forming unit erythroid (CFU-E) generation. CFU-E is the earliest stage of erythroid commitment from HSPCs. This effect was observed when canine BM cells were seeded in enriched methylcellulose media (Jones et al. 1979). However, the *in vitro* efficacy of canine EPO in mature erythroid cells remains unevaluated.

Given the growing demand for canine RBCs and the challenges associated with their *in vitro* production, this study aims to identify the optimal culture system for generating canine erythrocytes. Using specific culture conditions and monitoring relevant cell markers, we successfully stimulated canine MNCs to differentiate into RBCs *in vitro*. To our best knowledge, this is the first successful attempt of the *in vitro* production of canine erythrocytes, overcoming the challenges posed by the lack of suitable reagents and markers for dogs.

Materials and methods

Isolation of MNCs from canine peripheral blood (PB)

The Institutional Animal Care and Use Committee (IACUC) approved using Beagle peripheral blood. Whole blood was layered with Ficoll-Paque (1.078 g/mL, Cytiva, cat#17144003) in a 1:1 ratio in SepMate PBMNC isolation tubes (STEMCELL Technologies, cat#86450) and subjected to centrifugation at 500 × g for 35 min at room temperature. After centrifugation, the plasma supernatant and MNC layer were identified. The MNC layer was carefully collected, diluted in phosphate-buffered saline (PBS) containing 10% fetal bovine serum (FBS, HyClone™, cat#SH30071.03), and washed by centrifugation at 800 × g for 20 min at room temperature. The resulting cell pellets were collected to determine the total MNC count.

In vitro *erythroid differentiation of MNCs*

The isolated MNCs were cultured in StemSpan™ medium (STEMCELL Technologies, cat#09650) supplemented with 20–30% FBS and additional supplements. These supplements included holo-transferrin (200 ng/mL, Sigma-Aldrich, cat#T0665), insulin (10 μg/mL, Sigma-Aldrich, cat#I9278), penicillin–streptomycin (1%, Gibco), and antibiotic-antimycotic (1%, Gibco). The cultures were also supplemented with cytokines, including recombinant canine erythropoietin (cEPO) (10–160 ng/mL, R&D Systems, cat#3816-CE), recombinant human

erythropoietin (hEPO) (40–80 ng/mL, Millipore, cat#329871), recombinant canine stem cell factor (cSCF) (100 ng/mL, R&D Systems, cat#2278-SC), and recombinant human interleukin-3 (hIL-3) (10 ng/mL, R&D Systems, cat#203-IL). Concentrations of specific cytokines varied depending on the experimental design. A schematic of the workflow is shown in Graphical abstract.

Cell morphology analysis

Cultured erythroid lineage cells ($2–4 \times 10^4$) were smeared onto slides using a Cellspin cytocentrifuge and stained with Wright-Giemsa (Sigma-Aldrich, cat#w0625, cat#32884,). To distinguish the different erythroblast maturation stages and to quantify the proportions of each cell type in the cells derived from PB MNCs during *in vitro* erythropoiesis, cells cultured with 40 ng/mL cEPO were stained with Wright-Giemsa and analyzed microscopically. Cell sizes were assessed using ImageJ (version 1.54 g).

Quantitative real-time-polymerase chain reaction (qRT-PCR)

Total RNAs were collected from the 40 ng/mL cEPO-treated PB MNCs on day 0, during the early differentiation stages when the cell pellet began turning red (days 10–13), and during the later stages, when the proportion of enucleated erythrocytes increased, while cell viability remained between 60% and 80% (days 15–19). To assess gene expression during canine erythroid differentiation, qRT-PCR was performed using a 7500 Real-Time PCR System (Thermo Fisher Scientific). The mRNA expression levels were calculated by the $2-\triangle\triangle$Ct method (Bong et al. 2024). Canine glyceraldehyde 3-phosphate dehydrogenase (*GAPDH*) served as the loading control along with other erythroid markers; canine alpha hemoglobin stabilizing protein (*AHSP*) (Raess et al. 2012), canine Krüppel-like factor 1(*KLF1*) (Fanis et al. 2019), canine erythropoietin receptor (*EPOR*) (Bhoopalan et al. 2020), and canine transferrin receptor (*TFRC*) (Jia et al. 2020).

The primers (5′-3′) used for qRT-PCR were as follows:

- Canine *GAPDH*: F-aggtcggagtcaacggattt, R-tgactgtgccgtggaatttg
- Canine *AHSP*: F-tggaaactgtgggtgagaca, R-ccaccatttgctgcctgtaa
- Canine *KLF1*: F-agacacttgaagctcccaca, R-tgtaagctggtctgagggtc
- Canine *EPOR*: F-acagctagtgacttggaccc, R-aggccctcaaactcactctc
- Canine *TFRC*: F-ctttggacatgctcacctgg, R-atttcccaggcagaaggaca

Western blotting

Cultured cells were collected, washed with PBS, and lysed using a radioimmunoprecipitation assay (RIPA) buffer (Sigma-Aldrich, cat#R0278) (Kim et al. 2024). The extracted proteins were quantified using the Pierce BCA Protein Assay Kit (Thermo Fisher Scientific, cat#A55865) and separated by electrophoresis on a 10% sodium dodecyl sulfate-polyacrylamide gel electrophoresis (SDS-PAGE) gel. Proteins were transferred onto a polyvinylidene fluoride (PVDF) membrane (Invitrogen, cat#IB34001). The membrane was blocked with 5% skim milk and incubated with primary antibodies, i.e. anti-Hemoglobin α (1:1000, Abcam, cat#ab231732,) and anti-beta-actin (1:5000, Santa Cruze, cat#sc-47778,) (loading control antibody). Subsequently, the membrane was probed with secondary antibodies, i.e. anti-mouse IgG (Cell Signaling Technology, cat#7076) and anti-rabbit IgG (Cell Signaling Technology, cat#7074). Proteins were detected using the ChemiDoc XRS+ System (Bio-Rad).

Oxygen affinity of Hb

Approximately 1×10^7 cultured cells were collected as a cell pellet and resuspended in 2 mL Hemox solution buffer. As a control, 50 µL canine whole peripheral blood was prepared using the same method. Oxygen equilibrium curves were analyzed using a Hemox analyzer (TCS Medical Products Division).

Amino acid sequence and structure analysis

To analyze human and canine EPO, EPOR molecular graphics were performed with UCSF ChimeraX (Goddard et al. 2018). Sequence alignment of human and canine EPO and EPOR amino acids was conducted using Clustal Omega (Madeira et al. 2024)

Statistical analysis

Statistical significance was assessed using a non-parametric Student's *t*-test performed with using GraphPad Prism 10 (GraphPad). A *p*-value of ≤ 0.05 was considered statistically significant.

Results

Optimization of EPO concentrations in the culture medium for in vitro erythropoiesis of canine PB MNCs

As there are no prior studies on the *in vitro* erythroid differentiation of canine-derived cells, we adopted a

conventional culture system designed for the *in vitro* differentiation of human HSPCs (Bozhilov et al. 2023) to determine whether mature RBCs could be generated *in vitro* from canine PB MNCs. The culture medium was supplemented with specific erythropoietic cytokines, including hEPO, cSCF, and hIL-3, in addition to holo-transferrin and insulin.

The cytokine concentrations used for *in vitro* erythropoiesis were consistent with those established for human HSPCs, except for EPO. As the optimal concentration of cEPO for generating canine RBCs *in vitro* from PB MNCs has not been reported, we investigated the most appropriate concentration for the proliferation and differentiation of the erythroid lineage cells.

After isolating canine PB MNCs, the cells were seeded at a density of 1×10^6 cells/mL and monitored for proliferation and differentiation over three weeks. When the cells were cultured with varying concentrations of cEPO (10, 20, 40, 80, and 160 ng/mL), cell numbers initially decreased and stabilized around day 10 post-seeding, regardless of the cytokine concentration (Figure 1(a)). From day 0 to day 6, the proportion of seeded cells decreased by approximately 20%. Platelets present in the initial PB MNC population persisted for the first 6–7 days but gradually disappeared. Proliferation began thereafter, with an increase in total cell numbers. Enucleated erythrocytes were observed starting on day 10, and a red cell pellet formed (Figure 1(b)). The highest proliferation rate relative to the initial seeding of cells was observed by day 17, although donor variability influenced these rates (Figure 1(a)). Throughout the culture period, cell viability did not differ significantly among the groups.

Notably, the group supplemented with 40 ng/mL of cEPO showed the highest cell proliferation rate during the 17-day differentiation period (Figure 1(a)). However, no remarkable differences in proliferation rates were observed among the groups during the first seven days (Figure 1(a)). The proliferation rate declined when the cEPO concentration deviated from 40 ng/mL, either higher or lower (Figure 1(a)). Additional experiments using cEPO concentrations of 40 and 80 ng/mL (Figure 1(c)) or 30, 40, and 50 ng/mL (Figure 1(d)) confirmed that 40 ng/mL was the optimal concentration for maximizing cumulative cell numbers. These findings demonstrate that 40 ng/mL is the most effective concentration of cEPO for expanding PB MNCs into erythroid cells.

Remarkably, cEPO demonstrated higher efficacy than hEPO at promoting cell proliferation rates (Figure 1(c

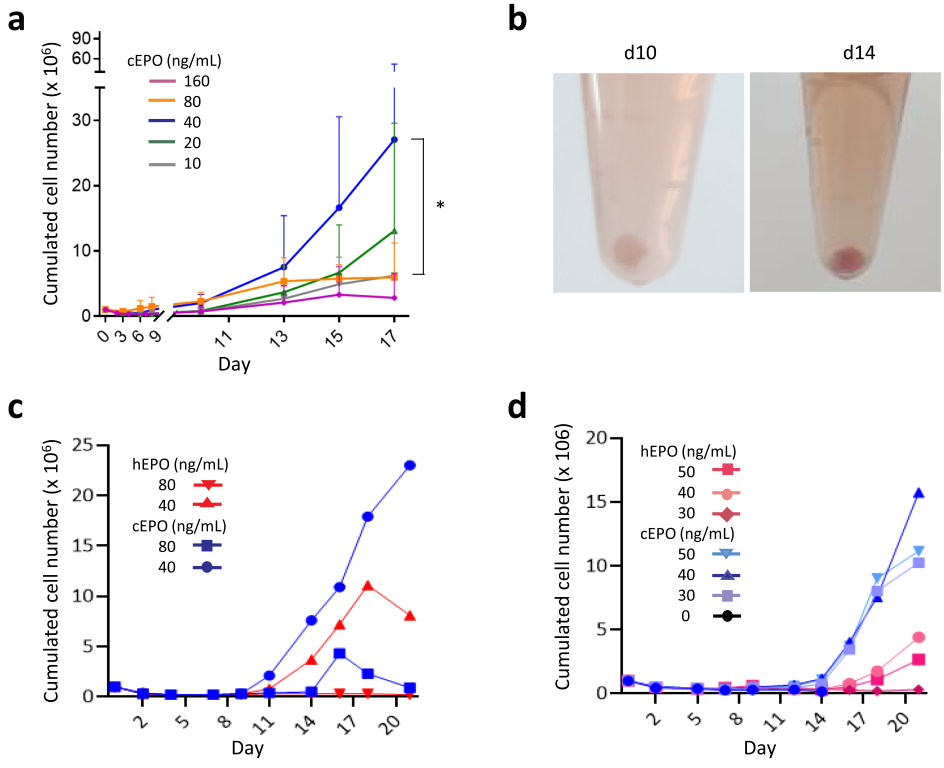

Figure 1. *In vitro* erythroid differentiation of canine PB MNCs with recombinant cEPO and recombinant hEPO. (a) Total cumulative cell numbers on differentiation days with cEPO at concentrations of 10 ng/mL ($n = 5$), 20 ng/mL ($n = 5$), 40 ng/mL ($n = 8$), 80 ng/mL ($n = 5$), and 160 ng/mL ($n = 2$). *Indicates statistical significance with $p \leq 0.05$. (b) Photographs of cell pellets on day 10 and day 14 of culture. (c) Total cumulative cell numbers with cEPO (40 and 80 ng/mL) compared to hEPO (40 and 80 ng/mL) ($n = 1$). (d) Total cumulative cell numbers with cEPO (30, 40, and 50 ng/mL) compared to those with hEPO (30, 40, and 50 ng/mL) ($n = 1$).

and d)). Although hEPO (40 ng/mL) also significantly promoted cell proliferation, the proliferation rates of cEPO-treated cells were 1.61- to 2.83-fold higher than those of hEPO-treated cells between days 18 and 21. These findings indicate that efficient *in vitro* expansion of erythroid lineage cells from canine PB MNCs can be achieved using the same cytokine cocktail used for human HSPC differentiation, with cEPO demonstrating significantly greater efficacy than hEPO at the optimal concentration of 40 ng/mL.

Canine erythropoiesis resembles human erythropoiesis and exhibits comparable morphological transitions of cells

When morphological characteristics and cell sizes were assessed using ImageJ, distinct erythroblast stages, ranging from proerythroblasts to mature RBCs, were identified (Figure 2(a and b)) and were comparable to those in humans, as described previously (England et al. 2011; Hedayanti and Wahyudi 2023). These findings indicate that the differentiation and maturation of canine erythroblasts can be categorized into distinct stages, similar to those observed in other mammalian cells. Notably, the cell diameters of the canine cells were smaller than those of the corresponding human cells at each differentiation stage, with the size disparity becoming more pronounced as differentiation progressed (Figure 2(b)).

To monitor the progression of erythroid differentiation in the presence of 40 ng/mL of cEPO, erythroblast numbers at specific differentiation stages were scored on particular days using morphological criteria. Prominent erythroid differentiation was observed starting on day 10, with gradual maturation, reaching 36.08% RBCs by day 17 (Figure 2(c)). These findings indicate that our *in vitro* differentiation protocol, supplemented with 40 ng/mL cEPO, effectively recapitulates *in vivo* erythropoiesis, similar to the protocols established for humans.

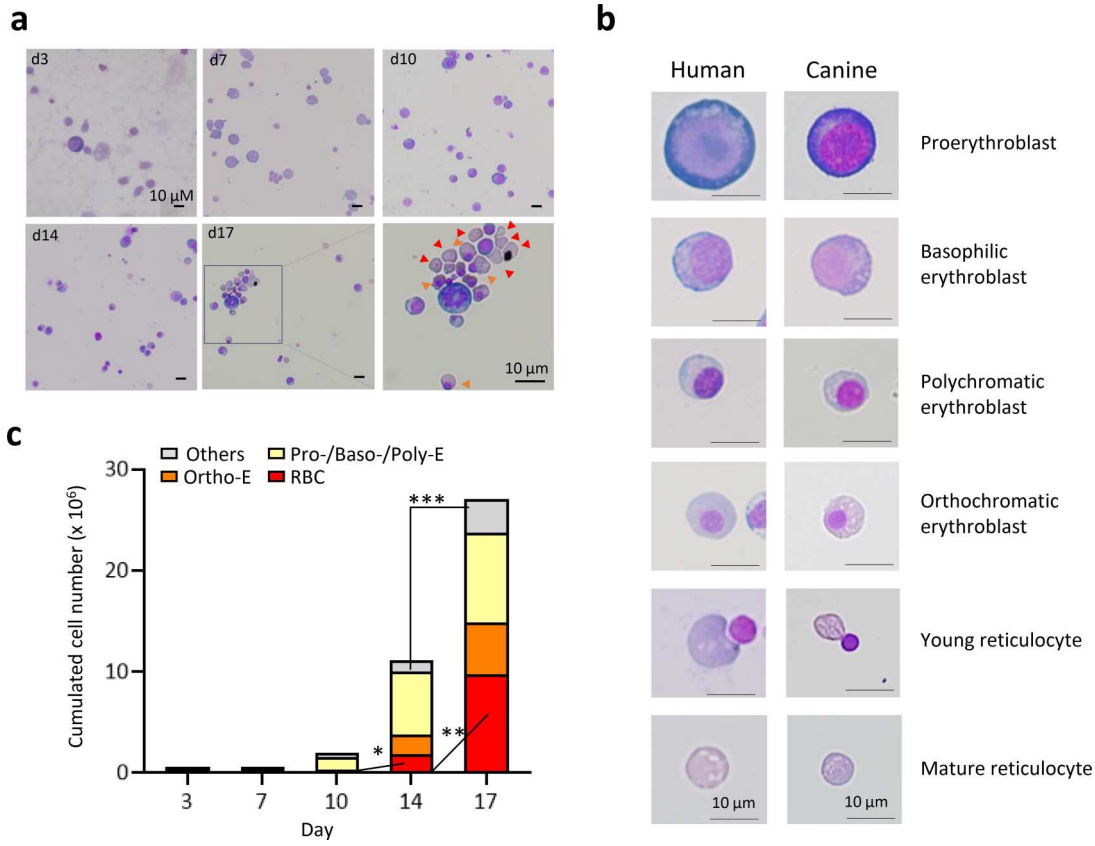

Figure 2. Characterization of cell types arising from *in vitro* erythroid differentiation of canine PB MNCs using cEPO at 40 ng/mL. (a) Representative Wright-Giemsa-stain images of cells during *in vitro* erythroid differentiation over 17 days. Orange arrowheads; Orthochromatic erythroblast, red arrowheads; Reticulocyte. (b) Identification of the major erythroid lineage cell types emerging from canine PB MNCs during *in vitro* differentiation, with a comparison to corresponding human cell types. (c) Quantification of cumulative erythroid lineage cell types during *in vitro* erythroid differentiation over 17 days. Erythroid cell types were quantified by counting over 200 cells per specific day of differentiation from Wright-Giemsa-stain images, and the stacked percentages of cell types were plotted. Scale bars: 10 μM. *$p \leq 0.05$, **$p \leq 0.01$, ***$p \leq 0.001$.

When erythroid cell types were quantified on day 17 for each cEPO concentration (in the samples shown in Figure 1(a)), erythroid maturation was found to be proportional to the percentage of cell expansion (Figure 3(a)). The highest level of erythroid differentiation was observed in the 40 ng/mL cEPO group

a

cEPO (ng/mL)	Maturation status	Mean ± SD (x 10^6 cells)
10 (n = 4)	RBC	1.065 ± 0.047
	Ortho-E	0.754 ± 0.022
	Pro-/Baso-/Poly-E	1.815 ± 0.130
	Others	2.711 ± 0.104
20 (n = 4)	RBC	2.700 ± 0.514
	Ortho-E	1.394 ± 0.338
	Pro-/Baso-/Poly-E	2.686 ± 0.834
	Others	6.315 ± 1.007
40 (n = 6)	RBC	9.765 ± 1.704
	Ortho-E	5.162 ± 1.276
	Pro-/Baso-/Poly-E	8.784 ± 1.241
	Others	3.350 ± 0.742
80 (n = 4)	RBC	1.882 ± 0.553
	Ortho-E	1.332 ± 0.218
	Pro-/Baso-/Poly-E	1.735 ± 0.439
	Others	0.996 ± 0.246
160 (n = 2)	RBC	1.027 ± 0.553
	Ortho-E	0.532 ± 0.171
	Pro-/Baso-/Poly-E	0.611 ± 0.157
	Others	0.658 ± 0.236

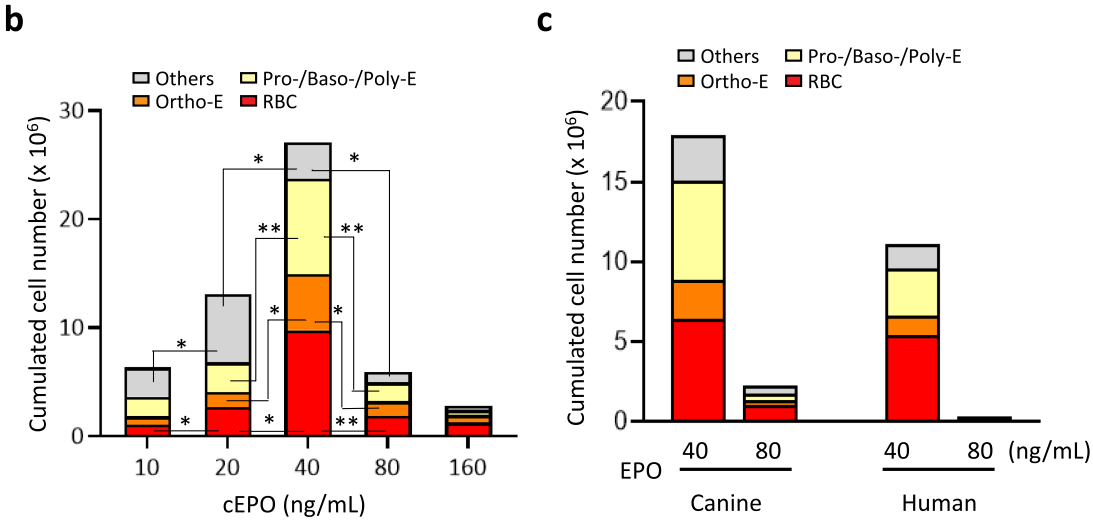

Figure 3. Quantification of cumulative erythroid lineage cell types during *in vitro* erythroid differentiation of canine PB MNCs with different concentrations of cEPO and hEPO. (a and b) Erythroid cell types on day 17 of the *in vitro* differentiation experiments presented in Figure 1a were quantified by counting over 200 cells for each specific concentration of cEPO from Wright-Giemsa-stain images. Quantification of cumulative erythroid lineage cell types with 10, 20, 40, 80 and 160 ng/mL of cEPO (a), and the stacked percentages of cell types (b). *$p \leq 0.05$, **$p \leq 0.01$, ***$p \leq 0.001$. (c) Stacked percentages of erythroid cell types with cEPO (40 and 80 ng/mL) compared to those with hEPO (40 and 80 ng/mL). Erythroid cell types on day 21 of the *in vitro* differentiation experiments presented in Figure 1(b) were quantified by counting over 100 cells for each specific concentration of cEPO and hEPO from Wright-Giemsa-stain images. RBC; red blood cells, Ortho-E; Ortho-erythroblasts, and Pro-/Baso-/Poly-E; pro-erythroblasts/baso-erythroblasts/poly-erythroblasts.

(Figure 3(a and b)). Similar to the proliferation rates, the erythroid differentiation rates declined when the cEPO concentration deviated from 40 ng/mL, either higher or lower. The mature RBC percentages in the 40 ng/mL group reached 36.08%, significantly higher than those observed in the 10 ng/mL (16.7%), 20 ng/mL (20.62%), 80 ng/mL (31.71%), and 160 ng/mL (14.6%) groups. Moreover, the proportion of differentiating erythroblasts was significantly higher in the 40 ng/mL cEPO-treated group than in the other cEPO concentration groups. These data demonstrate that the optimal cEPO concentration of 40 ng/mL is critical for the expansion, differentiation, and maturation of erythroid cells.

In contrast, 40 ng/mL hEPO induced erythroid cell maturation comparable to that observed for cEPO at the same concentration, although hEPO was less effective than cEPO in promoting erythroid cell expansion (Figure 3(c)). Notably, the percentage of mature RBCs in the 40 ng/mL hEPO-treated group was similar to that in the corresponding cEPO-treated group, despite a significantly reduced proportion of differentiating erythroblasts. These findings suggest that the binding of hEPO to cEPOR is the rate-limiting step, with normal erythroid differentiation proceeding thereafter.

Canine erythropoiesis resembles human erythropoiesis and exhibits comparable expression profiles of erythroid markers

Since no prior analyzes have examined erythroid marker expression during canine erythropoiesis, we sought to profile the mRNA expression of several

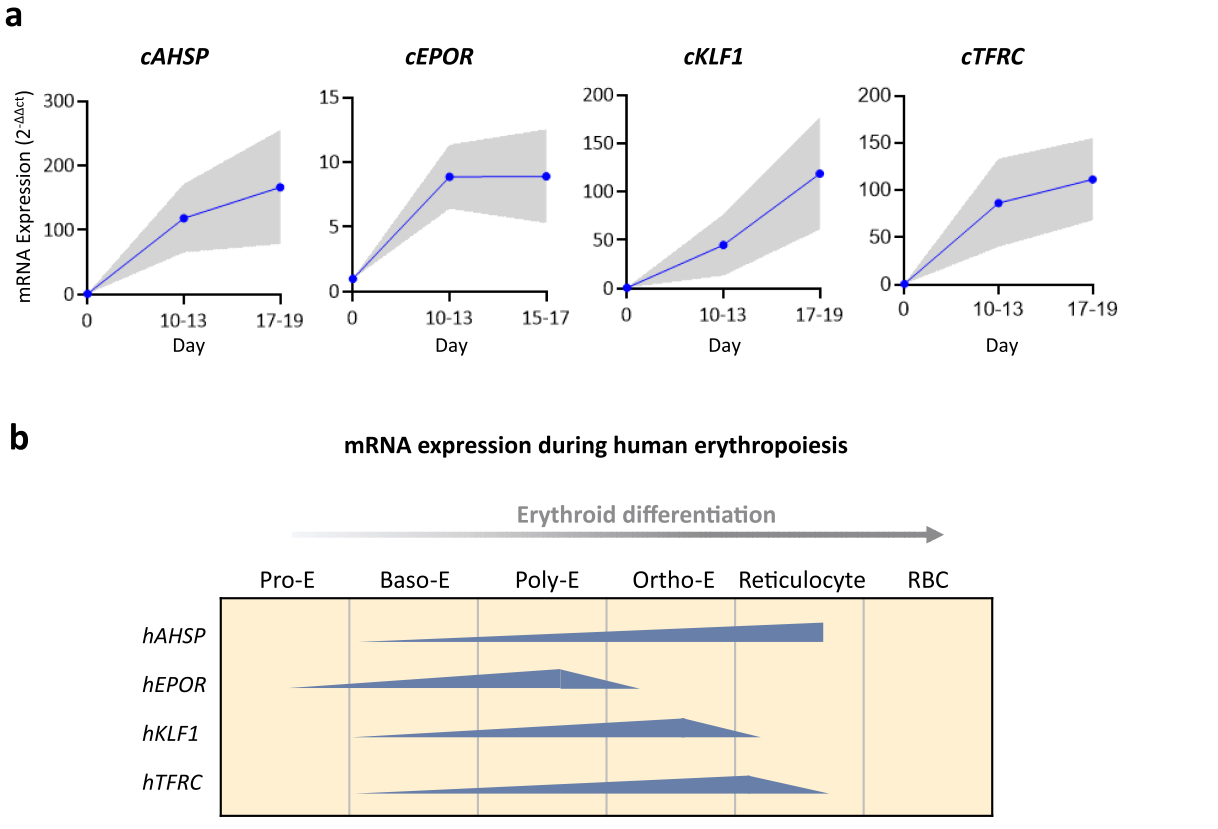

Figure 4. Expression profiles of erythroid differentiation marker genes during *in vitro* erythroid differentiation of canine PB MNCs with cEPO (40 ng/mL) over 3 weeks. (a) mRNA expression profiles of canine erythroid markers: canine alpha hemoglobin stabilizing protein (*cAHSP*; $n = 5$), canine Krüppel-like factor 1 (*cKLF1*; $n = 8$), canine erythropoietin receptor (*cEPOR*; $n = 6$), and canine transferrin receptor (*cTFRC*; n = 6). qRT-PCR was performed on total RNA extracted from specific days of differentiation, and the values (2^-ΔΔCt) were normalized to the expression levels at day 0. Blue lines represent the mean values, and the gray shades indicate the standard deviation (± SD). (b) A schematic representation of mRNA expression profiles of corresponding marker genes during human erythropoiesis. The mRNA expression data were obtained from previous studies (dos Santos et al. 2004; Marsee et al. 2010; Dzierzak and Philipsen 2013; Lee et al. 2023). It is noteworthy that *hAHSP* expression begins to increase in the baso-erythroblast stage, reaching its highest level in the reticulocyte. In contrast, *hEPOR* is expressed at the earliest stage of erythroid cell development, the proerythroblast, increases until the poly-erythroblast stage, but then starts to decrease and becomes undetectable in the reticulocyte. Although both *hKLF1* and *hTFRC* start to be expressed in the baso-erythroblast stage, *hKLF1* reaches its highest level in the ortho-erythroblast, while *hTFRC* peaks in the early reticulocyte stage.

erythroid-specific markers during the *in vitro* differentiation of canine PB MNCs in the presence of 40 ng/mL cEPO. However, establishing precise correlations was challenging due to limitations in the availability of canine RNA samples and donor variability among PB MNCs. Additionally, the presence of mixed hematopoietic lineage cells in differentiation cultures, along with reduced mRNA levels as erythrocytes underwent enucleation, made it difficult to identify significant trends in mRNA expression relative to culture dates and erythroid markers. Nevertheless, all four markers exhibited increased expression during the early stages (days 10–13). Among them, *cAHSP*, *cKLF1*, and *cTFRC* showed further increases during mature RBC formation, whereas *cEPOR* expression did not follow this trend (Figure 4(a)). By extrapolating the expression levels of each gene to the proportions of cell populations in Figure 2(c), we estimated the expression propensity of each gene during *in vitro* erythropoiesis. Since the proportion of polychromatic and orthochromatic erythroblasts was higher on day 17 than on days 10 or 14 in our *in vitro* differentiation experiments (Figure 2(c)), the expression profiles of *cAHSP*, *cKLF1*, and *cTFRC* closely resembled those observed in humans (dos Santos et al. 2004; Marsee et al. 2010; Dzierzak and Philipsen 2013; Lee et al. 2023) (Figure 4(b)). In contrast, *cEPOR* expression increased during the early stages (days 10–13) but did not show further increases in the later stages (days 15–17) (Figure 4(a)). Overall, our data indicate that canine erythropoiesis follows a pattern similar to that of human erythropoiesis, with comparable expression profiles of erythroid markers during the *in vitro* erythropoiesis of canine PB MNCs.

Erythroid cells derived from in vitro *differentiation of canine PB MNCs express mature hemoglobin with an oxygen-binding capacity comparable to that of* in vivo *RBCs*

To determine whether the erythroid cells derived from *in vitro* differentiation of canine PB MNCs, cultured with 40 ng/mL of cEPO, express functional mature hemoglobin, we assessed the expression level of hemoglobin α protein (HBA) in cells at day 21 of culture using western blot analysis. Compared to the RBCs prepared from canine PB, *in vitro* differentiated erythroid cells also expressed HBA (Figure 5(a)). Furthermore, when the oxygen equilibrium curve (Pan and Johnstone 1983) was established for the erythroid cells at day 18 using a Hemox analyzer, the analysis revealed a comparable p50 value to that of canine PB RBCs (21.03 mmHg for cultured cells versus 20.25 mmHg for peripheral RBCs; Figure. 5(b)). These findings demonstrate that

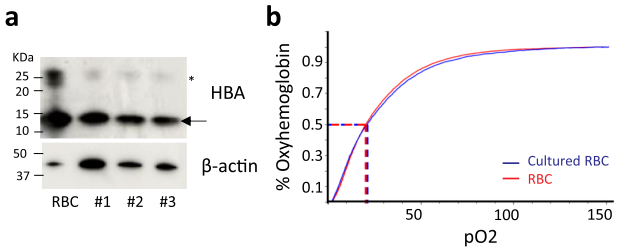

Figure 5. Functional analysis of day 17 cells from *in vitro* erythroid differentiation of canine PB MNCs with cEPO (40 ng/mL). (a) Western blot analysis of hemoglobin α (HBA) expression in differentiated cells from three different donors on day 21 of differentiation: lanes #1, #2, and #3. The lane labeled 'RBC' indicates peripheral blood RBCs collected from a reference dog. The arrow indicates the monomeric hemoglobin A (HBA), whereas the asterisk (*) denotes the HBA dimer. (b) Oxygen-binding capacity of the cells on day 18 of differentiation, demonstrating comparability to peripheral blood RBCs obtained from a different donor than the one used for *in vitro* differentiation.

erythroid cells generated *in vitro* express mature Hb with an oxygen-binding capacity similar to that of RBCs in canine PB.

Discussion

This study successfully established, for the first time, an *in vitro* canine RBC differentiation system. We characterized proliferation and differentiation of the cultured cells, and evaluated their functional properties. Initially, we attempted to isolate canine CD34+ cells from PB MNCs using methods similar to those used for human cells (Miharada et al. 2006; Lee et al. 2016) to differentiate them into a specific erythroid lineage. However, the attempt did not yield successful results and minimal proliferation was observed during the 7-day culture period (data not shown). Although the reagents were designated for canine use, they were less efficient than their human-specific counterparts. For instance, CD34+, a common marker used in sorting erythroid lineage cells from human PB MNCs, was unsuccessful. Furthermore, suitable canine markers, such as CD71 and CD235a for assessing erythroid cell maturity, were unavailable.

To address these challenges, we directly induced erythroid differentiation from canine PB MNCs by optimizing cytokine concentrations, enabling *in vitro* RBC production in dogs, analogous to that established human systems. The cytokine concentrations used for *in vitro* erythropoiesis were consistent with the protocols for human HSPCs, except for the EPO concentration optimization. We determined that 40 ng/mL cEPO was the optimal concentration for achieving the highest differentiation yield *in vitro*. In addition, cEPO

outperformed hEPO in this system. Both proliferation and erythroid differentiation rates declined with cEPO concentrations above or below this optimal value.

Our *in vitro* differentiation system, using 40 ng/mL of cEPO, efficiently promoted erythroid cell expansion, differentiation, and RBC maturation, as demonstrated by cell morphology, erythroid marker gene expression, and functional assays. We found distinct stages of canine erythroblast differentiation and maturation, mimicking those observed in mammalian cell systems. However, the cell diameters were smaller than those of the corresponding human cells at each stage of differentiation, with the size difference increasing throughout differentiation.

Several issues regarding the optimal EPO concentration for *in vitro* erythropoiesis in canine PB MNCs merit discussion. For instance, why do both proliferation and erythroid differentiation rates decline when the cEPO concentration deviates from this optimal value? EPO plays a dual role: first, it protects erythroid progenitors from apoptosis by activating anti-apoptotic proteins, including B-cell lymphoma-extra large (Bcl-XL). Second, it is essential for terminal differentiation by stimulating the expression of erythroid-specific transcription factors and genes, including Hb (Dolznig et al. 2002; Lee et al. 2016). Unlike the *in vivo* scenario, where feedback mechanisms tightly regulate EPO levels, *in vitro* erythropoiesis lacks such control. Suboptimal EPO concentrations may be insufficient to prevent apoptosis or stimulate mitosis in erythroid progenitor cells. Conversely, supra-optimal EPO concentrations may inhibit cell differentiation beyond the progenitor stage, potentially leading to cell death. This delicate balance underscores the necessity of maintaining an optimal EPO concentration to support both erythroid cell proliferation and differentiation.

Another point that warrants further discussion is the reason why the optimal concentration of EPO for *in vitro* differentiation of PB MNCs (i.e. 40 ng/mL) is approximately three times higher than that used for *in vitro* differentiation of CD34+ HSPCs (3 IU/mL, equivalent to 12.55 ng/mL; Merck cat#329871). A possible explanation is the continuous presence of the same EPO concentrations throughout the erythroid differentiation in our system, whereas EPO is typically withdrawn in the later stages of CD34+ HSPCs *in vitro* differentiation. This difference in protocol complicates comparisons between the two systems and highlights the need for further investigation into the factors influencing EPO concentration requirements.

Additionally, canine PB MNCs treated with cEPO (40 ng/mL) exhibited 1.61- to 2.83-fold higher proliferation and differentiation rates compared to those treated with hEPO (40 ng/mL). This difference can be attributed to species-specific interactions between EPO and EPOR, resulting in a higher affinity of cEPO for cEPOR than that of hEPO for cEPOR, despite similar biological activity across mammalian species. An important aspect of this interaction is the regulation of EPOR expression during erythroid development. In both humans and mice, EPOR expression has been reported to increase during the transition from burst-forming unit-erythroid (BFU-E) to colony-forming unit-erythroid (CFU-E) (Menon et al. 2006). Furthermore, studies using mouse models have demonstrated that EPOR expression gradually decreases during erythroblast maturation (Heinrich et al. 2004). This may influence the response to EPO during this critical developmental stage. The cEPO and hEPO share 81.21% identity and 93.93% similarity in their overall amino acid sequences, whereas cEPOR and hEPOR share 82.64% identity and 91.53% similarity. Notably, several amino acids involved in the EPO-EPOR interaction exhibit discrepancies in charge between canine and human EPO and EPOR (Figures 6 and 7). For instance, three residues in the D3 and D4 helices exhibit charge disparities, indicating structural differences between canine and human EPO (Figure 6). Additionally, a previous study reported that a critical hEPOR EPO-binding determinant (Phe93) resides in the L3 domain, as demonstrated by site-specific mutagenesis within the hEPOR extracellular domain (Middleton et al. 1996). In contrast, residues in the L5 domain contribute moderately or weakly to the binding of Phe93 to hEPO. Notably, in cEPOR, a charge difference in one L5 domain residue (His versus Leu) results in structural differences in the EPO-EPOR binding site three-dimensional model. This variation specifically affects the 1EBP structure for both EPOR and EPO mimics (Wen et al. 1994; Livnah et al. 1996) (Figure 7). These differences in the amino acid sequence of the L5 domain between hEPOR and cEPOR suggest potential variations in structural integrity, likely alter the binding affinities.

Our study had several limitations. First, further refinement of the *in vitro* erythroid differentiation procedures is required. This includes stepwise differentiation using cytokine combinations or coculture with stromal or mesenchymal stem cells, as suggested in recent human erythropoiesis studies (Bozhilov et al. 2023). Additionally, while we analyzed HBA expression and the p50 value for oxygen association-dissociation as functional indicators of erythrocytes, we found that canine RBCs derived from *in vitro* cultures closely resemble PB RBCs. However, our study has limitations in defining Hb types and fully characterizing RBC functionality. These limitations stem from the lack of specific antibodies and reagents for studying canine Hb, coupled with gaps in existing research. Further

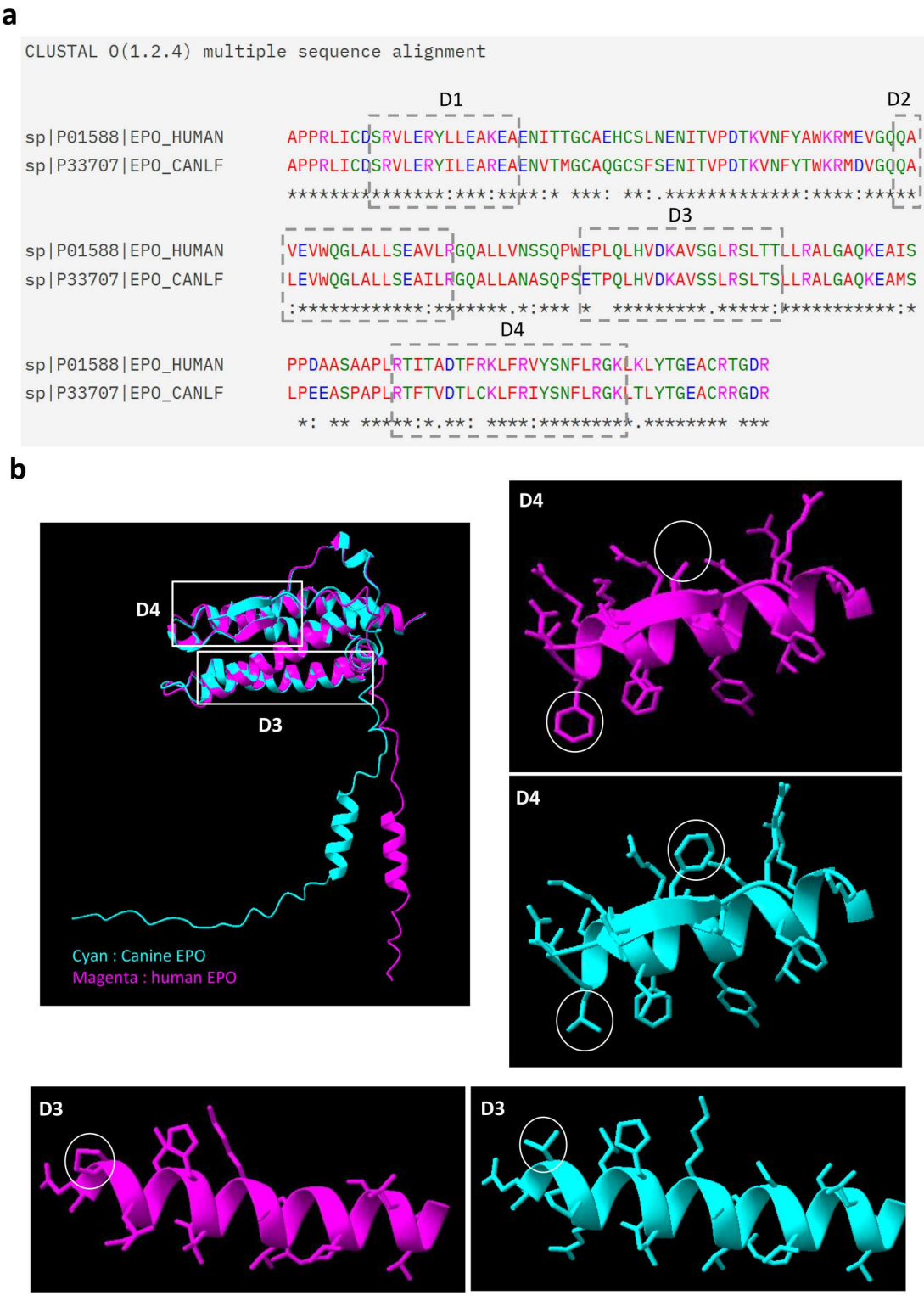

Figure 6. Structural differences between human and canine EPO. (a) Amino acid sequence alignment of mature human EPO (hEPO, P01588) and canine EPO (cEPO, P33707). Multiple sequence alignment was performed using Clustal Omega (PDB id: clustalo-I20241209-014629-0930-11133740-p1 m). The dotted square regions indicate the predicted amphipathic α-helical structures. (b) Aligned 3D structures of hEPO (magenta) and cEPO (cyan) in the D3 and D4 amphipathic α-helical regions, visualized using ChimeraX. The amino acid sequences of D3 (residues 89–107) are as follows: hEPO: EPLQLHVDKAVSGLRSLTT; cEPO: ETPQLHVDKAVSSLRSLTS. The amino acid sequences of D4 (residues 131–152) are as follows: hEPO: RTITADTFRKLFRVYSNFLRGK; cEPO: RTFTVDTLCKLFRIYSNFLRGK. Residues in a significant difference in three-dimensional structure are highlighted with white circles in the enlarged images.

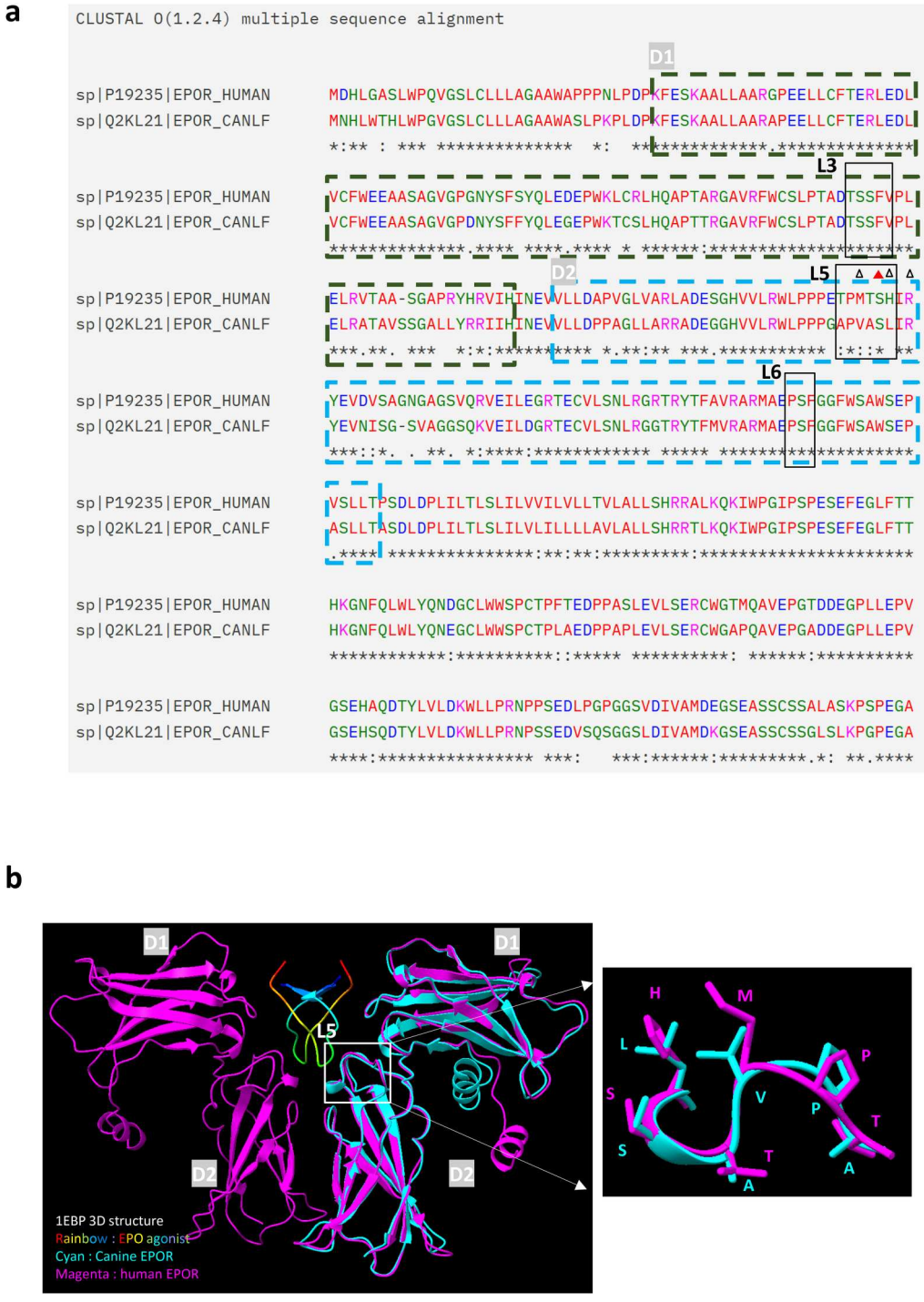

Figure 7. Structural differences between human and canine EPOR. (a) Amino acid sequence alignment of mature human EPOR (hEPOR, P19235) and canine EPOR (cEPOR, Q2KL21). Multiple sequence alignment was performed using Clustal Omega (PDB id: clustalo-I20241112-072919-0819-22641568-p1 m). The dotted square regions highlight predicted β-sheets around key EPO-binding loops (D1 and D2), where residues involving in hEPO binding are boxed with names; L3 (residues 90-94 in hEPOR: TSSFV), L5 (residues 148-153 in hEPOR: TPMTSH), and L6 (residues 203-205 in hEPOR: PSF). Residues in the L5 region affecting hEPO binding when mutated are marked with red (moderate) and blank (minor) triangles (Middleton et al. 1996). (b) Superposition of the extracellular domains of cEPOR (cyan) to those of hEPOR (magenta) in the three-dimensional structures of the extracellular binding domain (EPO-binding protein, EBP, residues 1–225 of the EPOR) and an EPO-mimetic peptide (EMP1) complex (1EBP) (Livnah et al. 1996). The cEPOR and hEPOR were superimposed only on their extracellular (D1 and D2) domains of one receptor monomer using ChimeraX. The L5 region (corresponding to residues 170–179) showing structural differences between hEPOR and cEPOR is enlarged on the right, where side chains are labeled for reference.

studies are essential to address these gaps and advance our understanding of this field, underscoring the importance of follow-up research.

In conclusion, we successfully established, for the first time, an *in vitro* erythroid differentiation system for canine PB MNCs, demonstrating the potential of *in vitro*-cultured canine RBCs for clinically advanced therapeutic applications.

Disclosure statement

No potential conflict of interest was reported by the author(s).

Funding

This work was funded by the Korean Government (Ministry of Science and ICT) under a National Research Foundation of Korea (NRF) and a Commercialization Promotion Agency for R&D Outcomes (COMPA) Grant (No. RS-2023-00236266).

References

Bhoopalan SV, Huang LJ-S, Weiss MJ. 2020. Erythropoietin regulation of red blood cell production: from bench to bedside and back. F. 1000R. es. 9:F1000 Faculty Rev-1153.

Bong D, Sohn J, Lee S-JV. 2024. Brief guide to RT-qPCR. Mol Cells. 47(12):100141. doi:10.1016/j.mocell.2024.100141.

Bozhilov YK, Hsu I, Brown EJ, Wilkinson AC. 2023. *In vitro* human haematopoietic stem cell expansion and differentiation. Cells. 12(6):896. doi:10.3390/cells12060896.

Brown JE, Adamson JW. 1977a. Modulation of *in vitro* erythropoiesis. The influence of beta-adrenergic agonists on erythroid colony formation. J Clin Invest. 60(1):70–77. doi:10.1172/JCI108771.

Brown JE, Adamson JW. 1977b. Modulation of *in vitro* erythropoiesis: enhancement of erythroid colony growth by cyclic nucleotides. Cell Tissue Kinet. 10(3):289–298.

Dolznig H, Habermann B, Stangl K, Deiner EM, Moriggl R, Beug H, Müllner EW. 2002. Apoptosis protection by the Epo target Bcl-X(L) allows factor-independent differentiation of primary erythroblasts. Curr Biol. 12(13):1076–1085. doi:10.1016/S0960-9822(02)00930-2.

dos Santos CO, Duarte ASS, Saad STO, Costa FF. 2004. Expression of α-hemoglobin stabilizing protein gene during human erythropoiesis. Exp Hematol. 32(2):157–162. doi:10.1016/j.exphem.2003.11.002.

Dzierzak E, Philipsen S. 2013. Erythropoiesis: development and differentiation. Cold Spring Harb Perspect Med. 3:a011601–a011601. doi:10.1101/cshperspect.a011601.

El Mahdy EM, Gamal M, Aboulhoda BE, Al Dreny BA, Shamaa A, Rashed L, Eldine Abdallah AN, Shamseldeen AM. 2023. Amelioration of rotenone-induced Parkinson's disease; comparing therapeutic role of erythropoietin versus low-level laser activation of mesenshymal stem cells (an in-vivo and in-vitro study). Anim Cells Syst (Seoul). 27(1):272-286. doi:10.1080/19768354.2023.2273467.

England SJ, McGrath KE, Frame JM, Palis J. 2011. Immature erythroblasts with extensive *ex vivo* self-renewal capacity emerge from the early mammalian fetus. Blood. 117(9):2708–2717. doi:10.1182/blood-2010-07-299743.

Fanis P, Kousiappa I, Phylactides M, Kyrri A, Hadjigavriel M, Christou S, Sitarou M, Kleanthous M. 2019. A novel mutation in the erythroid transcription factor KLF1 is likely responsible for ameliorating β-thalassemia major. Hum Mutat. 40(10):1768–1780. doi:10.1002/humu.23817.

Giarratana M-C, Rouard H, Dumont A, Kiger L, Safeukui I, Le Pennec P-Y, François S, Trugnan G, Peyrard T, Marie T, et al. 2011. Proof of principle for transfusion of *in vitro*–generated red blood cells. Blood. 118(19):5071–5079. doi:10.1182/blood-2011-06-362038.

Goddard TD, Huang CC, Meng EC, Pettersen EF, Couch GS, Morris JH, Ferrin TE. 2018. UCSF chimerax: meeting modern challenges in visualization and analysis. Protein Sci. 27:14–25. doi:10.1002/pro.3235.

Haase VH. 2010. Hypoxic regulation of erythropoiesis and iron metabolism. Am J Physiol Renal Physiol. 299(1):F1–F13. doi:10.1152/ajprenal.00174.2010.

Han SY, Lee EM, Lee J, Lee H, Kwon AM, Ryu KY, Choi WS, Baek EJ. 2021. Red cell manufacturing using parallel stirred-tank bioreactors at the final stages of differentiation enhances reticulocyte maturation. Biotechnol Bioeng. 118(5):1763–1778. doi:10.1002/bit.27691.

Hedayanti N, Wahyudi A. 2023. Review of physiological aspects of erythropoiesis: a narrative literature review. Sriwijaya J Intern Med. 1(1):19–25.

Heinrich AC, Pelanda R, Klingmüller U. 2004. A mouse model for visualization and conditional mutations in the erythroid lineage. Blood. 104(3):659–666. doi:10.1182/blood-2003-05-1442.

Jia S, Jia W, Yu S, Hu Y, He Y. 2020. Using microarray analysis to identify genes and pathways that regulate fetal hemoglobin levels. Ann Hum Genet. 84(1):29–36. doi:10.1111/ahg.12346.

Jones JB, Jolly JD, Dunn CD, Lange RD. 1979. The *in vitro* growth of erythroid colonies from dog bone marrow. Can J Comp Med. 43(4):365–370.

Kim S-W, Kim CW, Kim HS. 2024. Scoparone attenuates PD-L1 expression in human breast cancer cells by MKP-3 upregulation. Anim Cells Syst (Seoul). 28(1):55–65. doi:10.1080/19768354.2024.2315950.

Kutikuppala LVS, Ponnaganti SVK, Kale SSS, Kode R, Kuchana SK. 2023. Transfusions with laboratory-grown red blood cells: a new development in science. Exp. Hematol. 119–120:1-2.

Lee E, Han SY, Choi HS, Chun B, Hwang B, Baek EJ. 2015. Red blood cell generation by three-dimensional aggregate cultivation of late erythroblasts. Tissue Eng Part A. 21(3–4):817–828. doi:10.1089/ten.tea.2014.0325.

Lee SA, Kim JY, Choi Y, Kim Y, Kim HO. 2016. Application of mutant JAK2V617F for *in vitro* generation of red blood cells. Transfusion. 56(4):837–843. doi:10.1111/trf.13431.

Lee S-H, Shin D-J, Kim Y, Kim C-J, Lee J-J, Yoon MS, Uong TNT, Yu D, Jung J-Y, Cho D, et al. 2018. Comparison of phenotypic and functional characteristics between canine non-B, non-T natural killer lymphocytes and CD3+CD5dimCD21− cytotoxic large granular lymphocytes. Front Immunol. 9:841. doi:10.3389/fimmu.2018.00841.

Lee S-J, Jung C, Oh JE, Kim S, Lee S, Lee JY, Yoon YS. 2023. Generation of red blood cells from human pluripotent stem cells – an update. Cells. 12:1554.

Livnah O, Stura EA, Johnson DL, Middleton SA, Mulcahy LS, Wrighton NC, Dower WJ, Jolliffe LK, Wilson IA. 1996.

Functional mimicry of a protein hormone by a peptide agonist: the EPO receptor complex at 2.8Å. Science. 273(5274):464–471. doi:10.1126/science.273.5274.464.

Lykov AP, Surovtseva MA, Kim II, Bondarenko NA, Poveshchenko OV. 2020. Effect of erythro-poietin on morphofunctional properties of mesenchymalstem cells. Bull Exp Biol Med. 170:164–170. doi:10.1007/s10517-020-05024-z.

Madeira F, Madhusoodan N, Lee J, Eusebi A, Niewielska A, Tivey ARN, Lopez R, Butcher S. 2024. The EMBL-EBI job dispatcher sequence analysis tools framework in 2024. Nucleic Acids Res. 52:521–525. doi:10.1093/nar/gkae241.

Marsee DK, Pinkus GS, Yu H. 2010. CD71 (transferrin receptor): an effective marker for erythroid precursors in bone marrow biopsy specimens. Am J Clin Pathol. 134(3):429–435. doi:10.1309/AJCPCRK3MOAOJ6AT.

Menon MP, Fang J, Wojchowski DM. 2006. Core erythropoietin receptor signals for late erythroblast development. Blood. 107(7):2662–2672. doi:10.1182/blood-2005-02-0684.

Middleton SA, Johnson DL, Jin R, McMahon FJ, Collins A, Tullai J, Gruninger RH, Jolliffe LK, Mulcahy LS. 1996. Identification of a critical ligand binding determinant of the human erythropoietin receptor. Evidence for common ligand binding motifs in the cytokine receptor family. J Biol Chem. 271(24):14045–14054. doi:10.1074/jbc.271.24.14045.

Miharada K, Hiroyama T, Sudo K, Nagasawa T, Nakamura Y. 2006. Efficient enucleation of erythroblasts differentiated *in vitro* from hematopoietic stem and progenitor cells. Nat Biotechnol. 24(10):1255–1256. doi:10.1038/nbt1245.

Neildez-Nguyen TMA, Wajcman H, Marden MC, Bensidhoum M, Moncollin V, Giarratana MC, Kobari L, Thierry D, Douay L. 2002. Human erythroid cells produced *ex vivo* at large scale differentiate into red blood cells *in vivo*. Nat Biotechnol. 20(5):467–472. doi:10.1038/nbt0502-467.

Neuner E, Schumm M, Schneider EM, Guenther W, Ellwart J, Kremmer E, Vogl C, Buettner M, Thierfelder S, Kolb HJ. 1997. Immune phenotype of canine hematopoietic progenitor cells. Tissue Antigens. 50(5):466–474. doi:10.1111/j.1399-0039.1997.tb02901.x.

Niemeyer GP, Hudson J, Bridgman R, Spano J, Nash RA, Lothrop CD. 2001. Isolation and characterization of canine hematopoietic progenitor cells. Exp Hematol. 29(6):686–693. doi:10.1016/S0301-472X(01)00638-5.

Pan BT, Johnstone RM. 1983. Fate of the transferrin receptor during maturation of sheep reticulocytes *in vitro*: selective externalization of the receptor. Cell. 33(3):967–978. doi:10.1016/0092-8674(83)90040-5.

Popovic WJ, Brown JE, Adamson JW. 1977. The influence of thyroid hormones on *in vitro* erythropoiesis. Mediation by a receptor with beta adrenergic properties. J Clin Invest. 60(4):907–913. doi:10.1172/JCI108845.

Raess PW, Paessler ME, Bagg A, Weiss MJ, Choi JK. 2012. α-Hemoglobin-stabilizing protein is a sensitive and specific marker of erythroid precursors. Am J Surg Pathol. 36(10):1538–1547. doi:10.1097/PAS.0b013e31825fa501.

Stephenson JR, Axelrad AA, McLeod DL, Shreeve MM. 1971. Induction of colonies of hemoglobin-synthesizing cells by erythropoietin *in vitro*. Proc Natl Acad Sci U S A. 68(7):1542–1546. doi:10.1073/pnas.68.7.1542.

Suter SE, Gouthro TA, McSweeney PA, Nash RA, Haskins ME, Felsburg PJ, Henthorn PS. 2004. Isolation and characterization of pediatric canine bone marrow CD34+ cells. Vet Immunol Immunopathol. 101(1–2):31–47. doi:10.1016/j.vetimm.2004.03.009.

Wen D, Boissel JP, Showers M, Ruch BC, Bunn HF. 1994. Erythropoietin structure-function relationships. Identification of functionally important domains. J Biol Chem. 269(36):22839–22846. doi:10.1016/S0021-9258(17)31721-0.

Zhou S, Liu YG, Zhang Y, Hu JM, Liu D, Chen H, Li M, Guo Y, Fan LP, et al. 2018. Bone mesenchymal stem cells pretreatedwith erythropoietin enhance the effect to ameliorate cyclosporine A-induced nephrotoxicity in rats. J Cell Biochem. 119(10):8220–8232. doi:10.1002/jcb.26833.